Received: 13 December 2023 | Revised: 22 January 2024 | Accepted: 22 January 2024

DOI: 10.1111/joa.14022

Journal of Anatomy ANATOMICAL SOCIETY WILEY

METHOD

How to make a digital reconstruction of the human ribcage

José M. López-Rey[1,2] | Daniel García-Martínez[3,4,5] | Markus Bastir[1]

[1]Paleoanthropology Group, Department of Paleobiology, Museo Nacional de Ciencias Naturales (MNCN-CSIC), Madrid, Spain

[2]Department of Biology, Faculty of Sciences, Universidad Autónoma de Madrid (UAM), Madrid, Spain

[3]Physical Anthropology Unit, Department of Biodiversity, Ecology, and Evolution, Faculty of Biological Sciences, Universidad Complutense de Madrid (UCM), Madrid, Spain

[4]Laboratory of Forensic Anthropology, Centre for Functional Ecology, Department of Life Sciences, University of Coimbra (UC), Portugal

[5]Centro Nacional de Investigación sobre la Evolución Humana (CENIEH), Burgos, Spain

Correspondence
José M. López-Rey, Paleoanthropology Group, Department of Paleobiology, Museo Nacional de Ciencias Naturales (MNCN-CSIC), Madrid, Spain.
Email: jolopezr@mncn.csic.es

Funding information
Ministerio de Ciencia e Innovación, Grant/Award Number: PID2020-115854GB-I00 and PRE2021-097584

Abstract

Up to now, there have been no publication standardizing the digital reconstruction of the modern human ribcage from commingled costo-vertebral material. Consequently, we designed a validated protocol based on anatomical features observed in the literature and the CT scanned ribcages of 10 adult European individuals. After quantifying the shape of these ribcages using 3D geometric morphometrics, we split each vertebra and rib within their corresponding (semi)landmarks. Subsequently, individual bones + (semi)landmarks were imported to LhpFusionBox, commingled and 3D reconstructed. To validate the accuracy of the protocol, we first reconstructed a randomly chosen ribcage three times and then compared these reconstructions to the rest of the sample. Since these reconstructions were closer to their original counterpart than to the others, the remaining sample was reconstructed once. Next, we tested the intra-observer error during reconstructing using the Procrustes distances among the original ribcages and the reconstructions. We observed that first each ribcage reconstruction was clustered to its original counterpart and second there was a learning curve showing an improvement in the reconstruction process over time. Subsequently, we explored general size and shape differences among the original and reconstructed ribcages through a study of centroid size and a permutation test on the Procrustes distances (10,000 permutations), respectively. Specific shape differences between both groups were further examined through a principal component analysis in shape space. None of these analyses found statistical differences between the original and reconstructed ribcages ($p > 0.05$). Eventually, we extracted the mean shapes of the original ribcages and the reconstructions in order to visualize potential deviations caused by the anatomical considerations of the researcher. These results demonstrate that the protocol is accurate enough to be used when reconstructing a disarticulated human ribcage.

KEYWORDS
digital reconstruction, geometric morphometrics, modern human, ribcage, ribs, vertebrae

1 | INTRODUCTION

Traditionally, the study of the human post-cranial skeleton has been addressed from two different perspectives. On the one hand, bones have been described individually in order to list the particularities of their external and internal anatomy for easier sorting and identification (White & Folkens, 2005). On the other hand, anatomical regions such as the girdles or the extremities have been studied as a whole to link the anatomy of their constituent bones to their functionality (Gray, 1918; Spalteholz, 1970). In fact, there are metameric structures in the skeleton such as the spine or the ribcage where a holistic view of all the bones that compose them is necessary to understand their anatomical and functional dimensions.

Focusing on the ribs, there are plenty of studies that have found differences according to sex, age and/or eco-geographical location in *Homo sapiens* (Bellemare et al., 2006; Beresheim et al., 2019; García-Martínez et al., 2016, 2017; García-Martínez, Nalla, et al., 2018). In addition, although the anatomy, growth and functionality of the full ribcage has also been described in current humans (Bastir et al., 2013; Bellemare et al., 2003; García-Martínez, Bastir, Villa, et al., 2020; Graeber & Nazim, 2007; LoMauro & Aliverti, 2018), these publications sample a limited diversity of populations—as subjects are mainly from European ancestry—and dating—as the experiments are performed in vivo. Even though both issues could have been addressed by making studies on osteo-archaeological collections, there are certain difficulties based on the fact that vertebrae and mainly ribs, are very numerous and labile. Consequently, vertebral and costal series tend to appear incomplete, broken and/or commingled, so there have been few attempts to create 3D ribcage reconstructions in the literature.

The digital reconstruction of the human spine has already been discussed extensively in Been, Gómez-Olivencia, and Kramer (2019). In contrast, although there are some publications on reconstructing the full ribcage of several well-preserved fossil hominins (Bastir et al., 2020; García-Martínez, Bastir, Gómez-Olivencia, et al., 2020; Gómez-Olivencia et al., 2018), they do not detail nor standardize the methodology used for sorting and placing ribs over the spine. Furthermore, as stated by Sawyer and Maley (2005), ribcage reconstructions are subjective as long as they do not follow any protocol developed for that purpose. Given the important role played by the ribcage concerning hominin breathing kinematics, body proportions and locomotion (Bastir et al., 2020; Gea, 2008; Gómez-Olivencia et al., 2018; Latimer et al., 2016; Pomeroy, 2023; Torres-Tamayo et al., 2018), the aim of this article is to describe a standardized method for making a digital reconstruction of the modern human ribcage from commingled costo-vertebral remains, thus minimizing the artistic license observed in previous publications.

2 | MATERIALS AND METHODS

2.1 | Sample

The sample collected for making this protocol consisted of 10 healthy, adult, living individuals (5♀, 5♂) CT scanned at the Hospital Universitario La Paz (Madrid, Spain) in supine position at the total lung capacity (TLC) and residual volume (RV) (Wanger et al., 2005). Virtual ribcage models were segmented by standard methods in Slicer 4.10.2 software (www.slicer.org; Fedorov et al., 2012) using the module 'Grayscale Model Maker' and were then post-processed using Artec Studio 16 Professional and Geomagic Wrap 2021 (www.artec3d.com) for cleaning, smoothing edges and filling possible gaps. All image data were obtained with a 16-row multidetector CT scanner (Somatom Emotion 16, Siemens, Erlangen, Germany) with the following parameters: slice width, 0.3 mm; reconstruction increment, 0.5 mm; collimation, 16 × 0.75 mm; pitch, 0.8; slice collimation, 0.6 mm; voltage, 120 kVp; reference tube current–time, 160 mAs; and rotation time, 0.6 s. Routine matrix clinical images were reconstructed with a B41 kernel to an assessment of soft tissues and a high-resolution B90 kernel to an assessment of lung parenchyma. According to the Helsinki protocol (Goodyear et al., 2007), the study was approved by the institutional ethics committee (CEIC Hospital Universitario La Paz, HULP-PI-513) and all participants of this study signed a written consent that allowed the use of these data for scientific purposes.

2.2 | Anatomical study of the ribcage

The anatomy and 3D configuration of the modern human ribcage was studied using some well-known manuals (Gray, 1918; Spalteholz, 1970; White & Folkens, 2005). Since we planned to standardize our reconstructions at thoracic muscle relaxation—equivalent to functional residual capacity (FRC) (Wanger et al., 2005)—we observed general kinematic changes of the position of the ribs between TLC and RV using our sample of 10 individuals. The following list details the most important differences noticed between both breathing phases.

1. Sagittal inclination of the rib corpus: lower at TLC, being cranial ribs mostly perpendicular to the vertical axis of the spine.
2. Costovertebral articulation: The articular facets of the ribhead are dorsally retracted from the articular facets of the correspondent vertebral bodies at TLC and fully inserted at RV.
3. Costotransverse articulation: Barely changes, it is a fixed point for rib rotation during breathing.
4. Size of the intercostal spaces: Smaller at TLC. At RV, except at the most upper and lower costal levels, the intercostal spaces tend to have a height similar to the adjacent ribs in the sagittal plane.
5. Medio-lateral inclination of the ribhead: Although it changes relatively, the same pattern is followed at TLC and RV. Inclination decreases medially from upper to central ribs, which are horizontally-oriented. Then, inclination increases laterally from central to lower ribs.

Hence, in the reconstruction process, ribs were placed respecting what was observed at RV and avoiding positions similar to TLC. We also described specific characters present in the vertebrae and ribs for making their sorting easier in case the skeletal remains are commingled (Table 1).

2.3 | 3D geometric morphometrics

The shape of the original ribcages was quantified by 3D geometric morphometrics following the standard workflows stated by Bastir, García-Martínez, et al. (2019). To achieve that purpose, we imported the virtual models to Viewbox 4.0 (dHAL software, Kifissia, Greece) and measured them by a template of 526 (semi)landmarks, previously published (García-Martínez et al., 2019). The obtained coordinates were split into subsets belonging to individual bones for later analyses.

2.4 | Estimation of the missing parts

Given that the proposed method is meant to be used in osteo-archaeological collections, likely some of their vertebrae and/or ribs would be damaged or even missing. Therefore, it would be necessary to statistically estimate the missing elements such as done by García-Martínez, Riesco, and Bastir (2018), Bastir, Torres-Tamayo, et al. (2019) and Bastir et al. (2020).

2.5 | A software for 3D reconstruction: LhpFusionBox

Nowadays there are many software that allow the 3D reconstruction of anatomical regions. Among them, we chose LhpFusionBox (developed at the Université Libre de Bruxelles) not only because it is open access, but also because it easily allows the matching of (semi)landmarks to each mesh so that they can be moved together while reconstructing. This avoids intra-observer error introduced to repeated measurement of landmarks in the geometric morphometrics analyses of the reconstructions and their validations.

To make ribcage reconstructions using LhpFusionBox, we first have to import the rib and vertebrae meshes we want to work with (*File → Import → Geometries → choose format*) and set a screen for their proper view (*View → Add view → Surface*). Then we have to set the centroid of each mesh (*Operations → Create → Derive → Geometry centroid → click Centroid → vme → Explode*) and link it to a system of coordinates (*Operations → Create → Derive → AFRefsys → click AFRefsys → vme link PNT1, PNT2 and PNT3 to the exploded Centroid*). Next, we have to import the (semi)landmarks of interest (*File → Import → Motion analysis → Landmarks*) and link them to their corresponding mesh using Ctrl + R.

Once we have prepared the sample in the way detailed above, we have to select a mesh, press Ctrl + T and choose its previously settled system of coordinates (*Auxiliary ref sys → AFRefsys*). The mouse commands for working with the meshes are: left click (rotate), right click (zoom) and wheel click (scroll). When the meshes are in the required position, we can export them (*File → Export → Geometries → choose format*) and their linked landmarks (*File → Export → Motion analysis → Landmarks*). To make sure that our reconstruction protocol is accurate, we commingled the ribs and vertebrae of each individual before proceeding with the following methodology.

2.6 | Digital reconstruction of the thoracic spine

For reconstructing the thoracic spine, we used the 'zygapophyseal facet method' (ZAM; contiguity and maximal overlap of the zygapophyseal facets) described by Riesco López et al. (2018) and Bastir, Torres-Tamayo, et al. (2019). Since these publications highlighted that the ZAM may underestimate thoracic kyphosis, we corrected this technique by taking into consideration the wedging of

TABLE 1 Important characters to be considered when sorting commingled vertebrae and ribs.

Character	Observation
Vertebrae	
Dimensions of the vertebral body	Increase from T1 to T12
Orientation of the intervertebral discs	Less inclined ventrally from T1–T2 to T6–T7. Mostly horizontal from T7–T8 to T8–T9. More inclined dorsally from T9–T10 to T12–L1
Orientation of the spinous process	Horizontal or weakly inclined caudally in the upper and lower vertebrae. Evidently or strongly inclined caudally in the central vertebrae
Orientation of the transverse processes	Less inclined medially from T1 to T6. Mostly horizontal from T7 to T9. More inclined medially from T10 to T12
Orientation of the costo-vertebral facet joint	More cranial from T1 to T12
Ribs	
Length	Increases from R1 to R7/R8, then decreases to R12
Sagittal curvature of the rib corpus	Increases from R1 to R12
Medial curvature of the rib corpus	Decreases from R1 to R12
Distance between the tubercle and the costal angle	Increases from R1 to R12
Costal groove	Increases from R4 to R10. Barely pronounce or absent in the other levels
Position of the tubercle	Goes more caudal from R1 to R10. Tubercle is barely pronounce or absent in R11 and R12

the vertebral body. The obtained thoracic kyphosis was validated by a method based on the thoracic vertebral body height difference (TVBHD) presented by Goh et al. (1999) and Been, Waintraub, et al. (2019). To synthesize, the anterior and posterior vertebral body heights from T1 to T12 are measured and the sum of the anterior heights is divided between the sum of the posterior ones (A–P ratio). Then the A–P ratio is included in a regression formula (thoracic kyphosis in females = 428.756 – 411.87 × A–P ratio; thoracic kyphosis in males = 297.114 – 272.31 × A–P ratio) whose result is the approximate angle of thoracic kyphosis (average in modern humans = 50°). Measurements, calculations and graphic results are presented in Figure S1, and statistics are detailed in Table 2. Note that, in order to have a spatial reference to start the reconstruction, we always started with T8 and T9 since we observed that the intervertebral disc between both vertebrae is the one which corresponds most closely to the horizontal plane of a thorax in an anatomically meaningful orientation (Table 1).

2.7 | Digital reconstruction of the full ribcage

The reconstruction of the ribcage has several underlying issues to be addressed. Firstly, ribs have greater ranges of movement in the three corporal planes compared to vertebrae. In addition, despite of the fact that 'static' articular positions of the ribs could be defined by lung volumes (e.g. TLC, RV), these are relatively subjective since they depend on other organs and muscles rather than on the ribs themselves. This generates great difficulty when trying to rigorously standardize parameters like the costal inclination using regression formula such as done above for the spine. Therefore, as well as following the observations made for the position of the ribs at RV, we also based our method for ribcage reconstruction in maintaining continuity and symmetry. During reconstruction, transitions between ribs in the three corporal planes have to be smooth. Moreover, although alterations of bilateral symmetry were respected in the thoracic spine (e.g. scoliosis, different orientations of the transverse processes), ribs were placed as symmetrically as possible. These rules were followed by first placing the ribs from level 12 and then working towards the cranium on the already reconstructed spine because we noticed that the maximum rib inclination at thoracic muscle relaxation is mostly limited by the ribs of the lower thorax. The sternum was simply aligned to the distal ends of the ribs that articulate the manubrium and the sternal body.

2.8 | Statistical analyses

To validate the consistency of the proposed protocol and test the intra-observer error, we reconstructed a random ribcage (ID 1199748) three times on three different days and then we calculated the Procrustes distances among them and the rest of the original ribcage sample (Figure S2). Next, the remaining sample was reconstructed once. When we completed this process, we extracted the

TABLE 2 Statistical analyses performed in the study.

Test	Statistic	Thoracic kyphosis			Centroid size		PC1		PC2	
		Estimated	Original	Reconstruction	Original	Reconstruction	Original	Reconstruction	Original	Reconstruction
Shapiro–Wilk	W	0.983	0.955	0.972	0.86	0.89	0.926	0.91	0.914	0.844
	p	0.978	0.721	0.908	0.062	0.13	0.41	0.21	0.313	0.031
Student's *t*	t				-0.05		1.17			
	p				0.96		0.068			
Mann–Whitney U	w								67	
	p								0.674	
ANOVA	F	0.244								
	p	0.785								
Differences?		No			No		No		No	

Procrustes distances between the reconstructions and the originals with two main objectives. First, we clustered each reconstruction to the original ribcage sample to test whether it paired with its counterpart (Figure S3). Second, we created a learning curve to check if the accuracy of the reconstruction improved over time (Figure 1).

Once we validated the method by the previous procedures, we tested size and shape differences between the original and reconstructed ribcages. While general size differences between both groups were contrasted by Student's *t*-test of the centroid size (Table 2), general shape differences were studied using a permutation test (10,000 permutations) on the mean Procrustes distances between groups. Following, specific shape differences between the original ribcages and the reconstructions were calculated by a principal component analysis (PCA) in shape space and visualized along principal component (PC)1 and PC2 (Figure 2). A detailed depiction of the positive and negative shapes of PC1 (30.4% of total shape variation) is provided by Figure S4. Statistical differences between the original and reconstructed ribcages at PC1 and PC2 were evaluated as seen in Table 2. Lastly, we calculated the mean shapes of the original ribcages and the reconstructions in order to visualize potential deviations in the position of the ribs and vertebrae during the reconstruction process (Figure 3). All statistics were performed in R (R Core Team, 2017) using packages 'stats' 4.2.2 (R Core team), 'Morpho' 2.10, 'Rvcg' 0.22.1 (Schlager, 2017), 'geomorph' 4.04 (Adams et al., 2022), 'ggplot2' (Wickham, 2016) and 'cluster' (Maechler et al., 2022). The full R script is included in the Supplementary Online Material.

3 | RESULTS AND DISCUSSION

First, we tested the accuracy of the corrected ZAM using the TVBHD method. Differences between the thoracic kyphosis (°) of the original ribcages, the reconstructions and the TVBHD estimations were not significant ($p>0.05$), as can be seen in Table 2 and Figure S1. This confirms that the corrected ZAM is appropriate for accurate reconstructions of the thoracic spine. Statistical analyses demonstrated that the described method for reconstructing the full ribcage is efficient and results in 3D configurations are close to the originals. To begin with, the Procrustes distances of the three reconstructions of ID 1199748 are very similar among them and closer to the original ribcage than to the rest of the sample (Figure S2). Together with the fact that the biggest Procrustes distance among the three ID 1199748 reconstructions is much smaller than the lowest Procrustes distance among the original ribcage sample, we believe that intra-observer error had little impact on the reconstruction process. In addition, each reconstructed ribcage was paired to its corresponding original ribcage in the cluster analyses (Figure S3) and the learning curve showed that the accuracy of the method improves over time (Figure 1).

We also tested the precision of the protocol by making size and shape comparisons between the original and reconstructed ribcages. According to the centroid sizes (Table 2) and the permutation test ($p=0.795$), there were no statistical differences ($p>0.05$) between the size and shape of the original and reconstructed ribcages, respectively. Following this, specific shape differences were tested by a PCA (Figure 2). We did not find statistical differences ($p>0.05$) between both groups for PC1 and PC2 (57.2% of total shape variation) (Table 2).

These results support the consistency of the proposed reconstruction protocol. Nevertheless, the study of the mean shapes showed that this method is not perfect and depends on the anatomical considerations of the researcher (Sawyer & Maley, 2005). The superimposed mean shapes shown in Figure 3 do not fit perfectly because, during the reconstruction we first, overestimated the costal declination from level 6–9; second, overestimated the width of the upper thorax and underestimated that of the lower thorax; and third, slightly corrected scoliosis, which had an impact in the position of the lower left costal levels. Besides, the preservation of the skeletal material is another important limitation to be considered. Given that our protocol is highly based on specific anatomical features (Table 1), vertebrae and ribs for ribcage reconstruction should

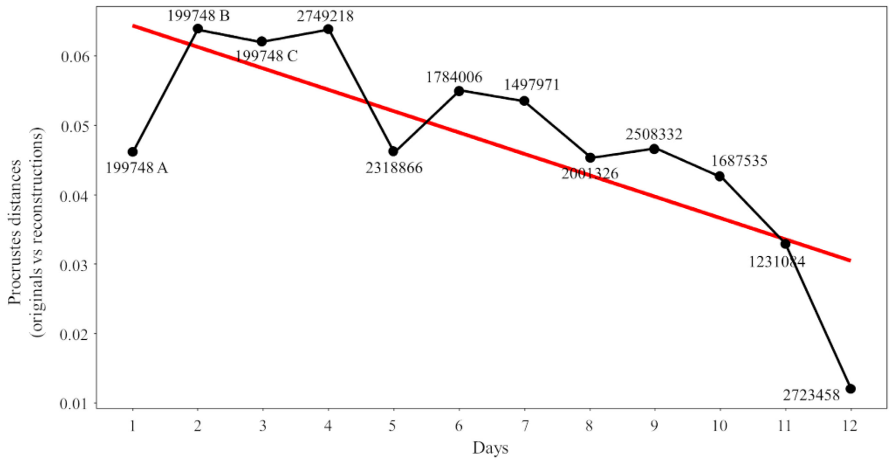

FIGURE 1 Learning curve showing the Procrustes distance among each original and reconstructed ribcage (*Y*-axis) over the days when each reconstruction was performed (*X*-axis). A tendency line is included in red.

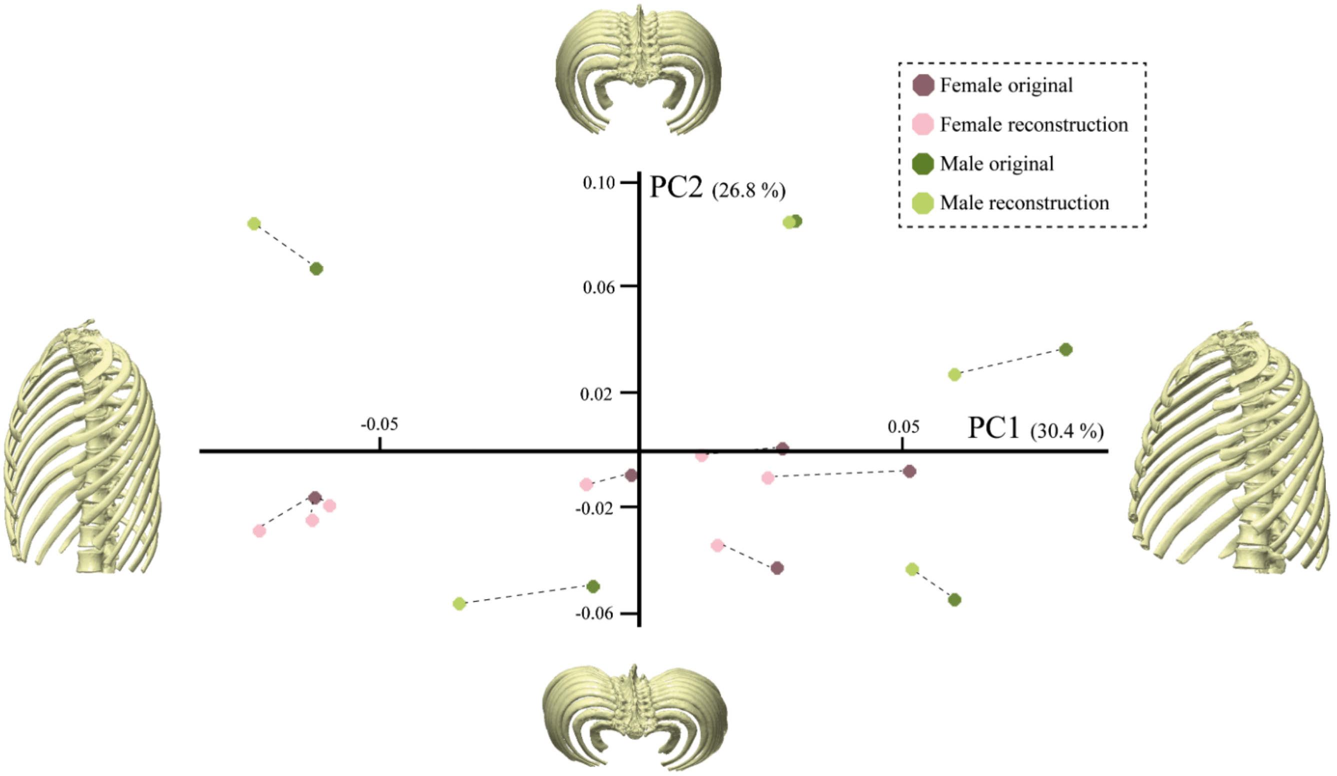

FIGURE 2 Scatterplot showing principal component (PC)1 and PC2. Each ribcage reconstruction is linked to its original counterpart. The accompanying visualizations show the shape of the ribcage at the extremes of both axes. Additionally, the percentage of explanation is indicated below each PC.

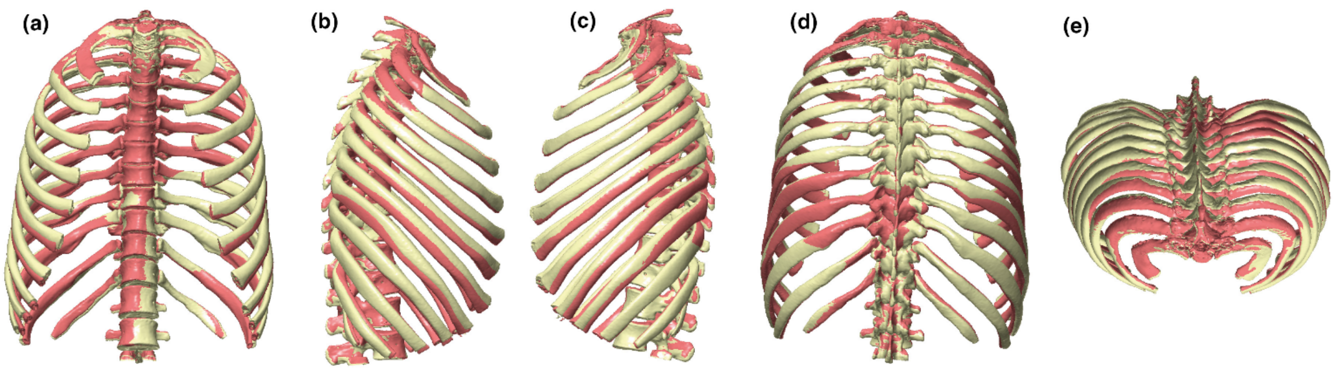

FIGURE 3 Superimposed mean shapes of the original (clear colour) and the reconstructed (pink, dark colour) ribcages in (a) frontal, (b) lateral right, (c) lateral left, (d) dorsal and (e) cranial view.

be chosen trying to keep these characteristics as much intact as possible. Fortunately, this can be addressed easily since there are publications where ribcage missing data have been estimated effectively (Bastir et al., 2020; Bastir, Torres-Tamayo, et al., 2019; García-Martínez, Riesco, & Bastir, 2018).

Given this, although this standardized protocol has only been tested in adult European *H. sapiens*, we propose that it would be applicable irrespective of the population of origin. Furthermore, adult fossil ribcages from exclusively bipedal hominins like *Homo neanderthalensis* and early *H. sapiens* would probably follow a pattern similar to that seen in current humans. Consequently, this protocol would be useful for standardizing ribcage reconstructions not only for modern human osteo-archaeological collections, but also for fossil hominins. There are, however, some constraints in applying this method to non-adult individuals. Despite the fact that ontogenetic changes have already been described in the modern human ribcage (Bastir et al., 2013; Scheuer & Black, 2000), the great variability in the degree of ossification at each costal and vertebral level makes it complicated to standardize ribcage reconstruction in non-adult individuals. In any case, it would be necessary to conduct a study for different age ranges in order to achieve standardization. This would be interesting for future analyses, not only about the ontogenetic study of the modern human ribcage but also about fossils such as KNM-WT 15000 (Bastir et al., 2020) or Dederiyeh 1 (García-Martínez, Bastir, Gómez-Olivencia, et al., 2020).

AUTHOR CONTRIBUTIONS

José M. López-Rey: design of the experiment, data analysis, data interpretation and drafting of the manuscript. **Daniel García-Martínez**: design of the experiment, data analysis, data interpretation, critical revision of the manuscript and approval of the article. **Markus Bastir**: design of the experiment, acquisition of data, data analysis, data interpretation, critical revision of the manuscript and approval of the article. **Marta Gómez-Recio**: figure design and statistics. **Daniel Sanz-Prieto**: statistics. **Carlos A. Palancar**: statistics. **Isabel Torres-Sánchez**: acquisition of data. **Francisco García-Río**: acquisition of data.

ACKNOWLEDGEMENTS

We would like to acknowledge Marta Gómez-Recio for her valuable recommendations during the figure editing process. Additionally, we extend our thanks to Daniel Sanz-Prieto and Dr. Carlos A. Palancar for their advice on statistical analyses and specific functionalities of LhpFusionBox. Finally, we would like to acknowledge the contributions of Dr. Isabel Torres-Sánchez and Dr. Francisco García-Río for providing the CT data. The Spanish Ministry of Science and Innovation funds this research by a Plan Nacional project to MB (reference: PID2020-115854GB-100) and a predoctoral fellowship to JMLR (reference: PRE2021-097584). All the authors state that there are no conflicts of interest.

DATA AVAILABILITY STATEMENT

The data that support the findings of this study are available upon reasonable request from the corresponding author. The data are not publicly available due to privacy or ethical restrictions.

ORCID

José M. López-Rey https://orcid.org/0000-0002-0148-5666
Daniel García-Martínez https://orcid.org/0000-0001-7518-3866
Markus Bastir https://orcid.org/0000-0002-3141-3401

REFERENCES

Adams, D., Collyer, M., Kaliontzopoulou, A. & Baken, E. (2022) Geomorph: software for geometric morphometric analyses. R Package Version 4.0.4. Available from: https://cran.r-project.org/package=geomorph

Bastir, M., García Martínez, D., Recheis, W., Barash, A., Coquerelle, M., Rios, L. et al. (2013) Differential growth and development of the upper and lower human thorax. *PLoS One*, 8(9), e75128. Available from: https://doi.org/10.1371/journal.pone.0075128

Bastir, M., García-Martínez, D., Torres-Tamayo, N., Palancar, C.A., Beyer, B., Barash, A. et al. (2020) Rib cage anatomy in *Homo erectus* suggests a recent evolutionary origin of modern human body shape. *Nature Ecology & Evolution*, 4(9), 1178–1187. Available from: https://doi.org/10.1038/s41559-020-1240-4

Bastir, M., García-Martínez, D., Torres-Tamayo, N., Palancar, C.A., Fernández-Pérez, F.J., Riesco-López, A. et al. (2019) Workflows in a virtual morphology lab: 3D scanning, measuring, and printing. *Journal of Anthropological Sciences*, 97, 107–134. Available from: https://doi.org/10.4436/jass.97003

Bastir, M., Torres-Tamayo, N., Palancar, C.A., Lois-Zlolniski, S., García-Martínez, D., Riesco-López, A. et al. (2019) Geometric morphometric studies in the human spine. In: Been, E., Gómez-Olivencia, A. & Kramer, P.A. (Eds.) *Spinal evolution: morphology, function, and pathology of the spine in hominoid evolution*. Cham, Switzerland: Springer, pp. 361–386.

Been, E., Gómez-Olivencia, A. & Kramer, P.A. (Eds.). (2019) *Spinal evolution: morphology, function, and pathology of the spine in hominoid evolution*. Cham, Switzerland: Springer.

Been, E., Waintraub, T., Gómez-Olivencia, A., Kalichman, L., Kramer, P.A., Shefi, S. et al. (2019) How to build a 3D model of a fossil hominin vertebral spine based on osseous material. In: Been, E., Gómez-Olivencia, A. & Kramer, P.A. (Eds.) *Spinal evolution: morphology, function, and pathology of the spine in hominoid evolution*. Cham, Switzerland: Springer, pp. 341–360.

Bellemare, F., Fuamba, T. & Bourgeault, A. (2006) Sexual dimorphism of human ribs. *Respiratory Physiology & Neurobiology*, 150(2–3), 233–239. Available from: https://doi.org/10.1016/j.resp.2005.04.002

Bellemare, F., Jeanneret, A. & Couture, J. (2003) Sex differences in thoracic dimensions and configuration. *American Journal of Respiratory and Critical Care Medicine*, 168(3), 305–312. Available from: https://doi.org/10.1164/rccm.200208-876OC

Beresheim, A.C., Pfeiffer, S. & Grynpas, M. (2019) Ontogenetic changes to bone microstructure in an archaeologically derived sample of human ribs. *Journal of Anatomy*, 236(3), 448–462. Available from: https://doi.org/10.1111/joa.13116

Fedorov, A., Beichel, R., Kalpathy-Cramer, J., Finet, J., Fillion-Robin, J.C., Pujol, S. et al. (2012) 3D Slicer as an image computing platform for the Quantitative Imaging Network. *Magnetic Resonance Imaging*, 30(9), 1323–1341. Available from: https://doi.org/10.1016/j.mri.2012.05.001

García-Martínez, D., Bastir, M., Gómez-Olivencia, A., Maureille, B., Golovanova, L., Doronichev, V. et al. (2020) Early development of the Neanderthal ribcage reveals a different body shape at birth compared to modern humans. *Science Advances*, 6(41), eabb4377. Available from: https://doi.org/10.1126/sciadv.abb4377

García-Martínez, D., Bastir, M., Torres-Tamayo, N., O'Higgins, P., Torres-Sánchez, I., García-Río, F. et al. (2019) Three-dimensional analysis of sexual dimorphism in ribcage kinematics of modern humans. *American Journal of Physical Anthropology*, 169(2), 348–355. Available from: https://doi.org/10.1002/ajpa.23829

García-Martínez, D., Bastir, M., Villa, C., García-Río, F., Torres-Sánchez, I., Recheis, W. et al. (2020) Late subadult ontogeny and adult aging of the human thorax reveals divergent growth trajectories between sexes. *Scientific Reports*, 10(1), 10737. Available from: https://doi.org/10.1038/s41598-020-67664-5

García-Martínez, D., Gil, O.G., Cambra-Moo, O., Canillas, M., Rodríguez, M.A., Bastir, M. et al. (2017) External and internal ontogenetic changes in the first rib. *American Journal of Physical Anthropology*, 164(4), 750–762. Available from: https://doi.org/10.1002/ajpa.23313

García-Martínez, D., Nalla, S., Ferreira, M.T., Guichón, R.A., D'Angelo del Campo, M.D. & Bastir, M. (2018) Eco-geographic adaptations in the human ribcage throughout a 3D geometric morphometric approach. *American Journal of Physical Anthropology*, 166(2), 323–336. Available from: https://doi.org/10.1002/ajpa.23433

García-Martínez, D., Recheis, W. & Bastir, M. (2016) Ontogeny of 3D rib curvature and its importance for the understanding of human thorax development. *American Journal of Physical Anthropology*, 159(3), 423–431. Available from: https://doi.org/10.1002/ajpa.22893

García-Martínez, D., Riesco, A. & Bastir, M. (2018) Missing element estimation in sequential anatomical structures: the case of the human thoracic vertebrae and its potential application to the fossil record. In: Rissech, C., Nadal, J. & Fullola, J.M. (Eds.) *Geometric morphometrics: trends in biology, paleobiology and archaeology*. Barcelona: Seminari d'Estudis i Recerques Preshistoriques, Universitat de Barcelona (SERP), Societat Catalana d'Arqueologia (SCA), pp. 93–97.

Gea, J. (2008) The evolution of the human species: a long journey for the respiratory system. *Archivos de Bronconeumología (English Edition)*, 44(5), 263–270. Available from: https://doi.org/10.1016/S1579-2129(08)60042-7

Goh, S., Price, R.I., Leedman, P.J. & Singer, K.P. (1999) The relative influence of vertebral body and intervertebral disc shape on thoracic kyphosis. *Clinical Biomechanics*, 14(7), 439–448. Available from: https://doi.org/10.1016/S0268-0033(98)00105-3

Gómez-Olivencia, A., Barash, A., García-Martínez, D., Arlegi, M., Kramer, P., Bastir, M. et al. (2018) 3D virtual reconstruction of the Kebara 2 Neandertal thorax. *Nature Communications*, 9(1), 1–8. Available from: https://doi.org/10.1038/s41467-018-06803-z

Goodyear, M.D., Krleza-Jeric, K. & Lemmens, T. (2007) The declaration of Helsinki. *BMJ*, 335(7621), 624–625. Available from: https://doi.org/10.1136/bmj.39339.610000.BE

Graeber, G.M. & Nazim, M. (2007) The anatomy of the ribs and the sternum and their relationship to chest wall structure and function. *Thoracic Surgery Clinics*, 17(4), 473–489. Available from: https://doi.org/10.1016/j.thorsurg.2006.12.010

Gray, H. (1918) *Anatomy of the human body*. Philadelphia: Lea & Febiger.

Latimer, B.M., Lovejoy, C.O., Spurlock, L. & Haile-Selassie, Y. (2016) The thoracic cage of KSD-VP-1/1. In: Haile-Selassie, Y. & Su, D.F. (Eds.) *The postcranial anatomy of Australopithecus afarensis*. Dordrecht: Springer, pp. 143–153.

LoMauro, A. & Aliverti, A. (2018) Sex differences in respiratory function, 14(2), 131–140. Available from: https://doi.org/10.1183/20734735.000318

Maechler, M., Rousseeuw, P., Struyf, A., Hubert, M. & Hornik, K. (2022) Cluster: cluster analysis basics and extensions. R Package Version 2.1.4. Available from: https://CRAN.R-project.org/package=cluster

Pomeroy, E. (2023) The different adaptive trajectories in Neanderthals and *Homo sapiens* and their implications for contemporary human physiological variation. *Comparative Biochemistry and Physiology Part A: Molecular & Integrative Physiology*, 280, 111420. Available from: https://doi.org/10.1016/j.cbpa.2023.111420

R Core Team. (2017) *R: a language and environment for statistical computing*. Vienna, Austria: R Foundation for Statistical Computing.

Riesco López, A., García-Martínez, D. & Bastir, M. (2018) Reconstrucción del segmento torácico de la columna vertebral en Paleoantropología. In: Amayuelas, E., Bilbao-Lasa, P., Bonitlla, O., del Val, M., Errandonea-Martín, J., Garate-Olave, I. et al. (Eds.) *Life finds a way*. Gasteiz: Encuentro de Jóvenes investigadores en Paleontología, pp. 241–244.

Sawyer, G.J. & Maley, B. (2005) Neanderthal reconstructed. *The Anatomical Record*, 283(1), 23–31. Available from: https://doi.org/10.1002/ar.b.20057

Scheuer, L. & Black, S. (2000) *Developmental juvenile osteology*. San Diego: Elsevier.

Schlager, S. (2017) Morpho and Rvcg–shape analysis in R: R-packages for geometric morphometrics, shape analysis, and surface manipulations. In: Zheng, G., Li, S. & Székely, G. (Eds.) *Statistical shape and deformation analysis*. Cambridge (Massachusetts): Academic Press, pp. 217–256.

Spalteholz, W. (1970) *Handatlas der Anatomie des Menschen*, Spanish edition. Barcelona: Editorial Labor.

Torres-Tamayo, N., García-Martínez, D., Nalla, S., Barash, A., Williams, S.A., Blanco-Pérez, E. et al. (2018) The torso integration hypothesis revisited in *Homo sapiens*: contributions to the understanding of hominin body shape evolution. *American Journal of Physical Anthropology*, 167(4), 777–790. Available from: https://doi.org/10.1002/ajpa.23705

Wanger, J., Clausen, J.L., Coates, A., Pedersen, O.F., Brusasco, V., Burgos, F. et al. (2005) Standardisation of the measurement of lung volumes. *European Respiratory Journal*, 26(3), 511–522. Available from: https://doi.org/10.1183/09031936.05.00035005

White, T.D. & Folkens, P.A. (2005) *The human bone manual*. San Diego: Elsevier.

Wickham, H. (2016) *ggplot2: elegant graphics for data analysis*. New York: Springer-Verlag. ISBN 978-3-319-24277-4. Available from: https://ggplot2.tidyverse.org

SUPPORTING INFORMATION

Additional supporting information can be found online in the Supporting Information section at the end of this article.

How to cite this article: López-Rey, J.M., García-Martínez, D. & Bastir, M. (2024) How to make a digital reconstruction of the human ribcage. *Journal of Anatomy*, 245, 27–34. Available from: https://doi.org/10.1111/joa.14022